

269
11-13-79

DR 277

LA-7885-MS, Vol. II

Informal Report

**1-GWh Diurnal Load-Leveling Superconducting
Magnetic Energy Storage System Reference Design**

Appendix A: Energy Storage Coil and Superconductor

University of California

MASTER



LOS ALAMOS SCIENTIFIC LABORATORY

Post Office Box 1663 Los Alamos, New Mexico 87545

DISTRIBUTION OF THIS DOCUMENT IS UNLIMITED

MASTER

LA-7885-MS, Vol. II
Informal Report
UC-20b and UC-94b
Issued: September 1979

1-GWh Diurnal Load-Leveling Superconducting Magnetic Energy Storage System Reference Design

Appendix A: Energy Storage Coil and Superconductor

R. I. Schermer

MASTER

DISCLAIMER

This document contains information that is proprietary to Lockheed Martin Energy Research Corporation (LM-ERCO). It is the property of LM-ERCO and is loaned to you. It and its contents are not to be distributed outside your organization. It is to be used only for the purposes for which it was loaned to you. It is not to be retransmitted, copied, or otherwise disseminated without the express written permission of LM-ERCO. If you are not an employee of LM-ERCO, you are not to disseminate this information to any other person. If you are an employee of LM-ERCO, you are not to disseminate this information to any other person without the express written permission of LM-ERCO. If you are a contractor of LM-ERCO, you are not to disseminate this information to any other person without the express written permission of LM-ERCO. If you are a subcontractor of LM-ERCO, you are not to disseminate this information to any other person without the express written permission of LM-ERCO. If you are a consultant of LM-ERCO, you are not to disseminate this information to any other person without the express written permission of LM-ERCO. If you are a vendor of LM-ERCO, you are not to disseminate this information to any other person without the express written permission of LM-ERCO. If you are a customer of LM-ERCO, you are not to disseminate this information to any other person without the express written permission of LM-ERCO. If you are a licensee of LM-ERCO, you are not to disseminate this information to any other person without the express written permission of LM-ERCO. If you are a partner of LM-ERCO, you are not to disseminate this information to any other person without the express written permission of LM-ERCO. If you are a joint venturer of LM-ERCO, you are not to disseminate this information to any other person without the express written permission of LM-ERCO. If you are a member of LM-ERCO, you are not to disseminate this information to any other person without the express written permission of LM-ERCO. If you are an officer or director of LM-ERCO, you are not to disseminate this information to any other person without the express written permission of LM-ERCO. If you are an employee of LM-ERCO, you are not to disseminate this information to any other person without the express written permission of LM-ERCO. If you are a contractor of LM-ERCO, you are not to disseminate this information to any other person without the express written permission of LM-ERCO. If you are a subcontractor of LM-ERCO, you are not to disseminate this information to any other person without the express written permission of LM-ERCO. If you are a consultant of LM-ERCO, you are not to disseminate this information to any other person without the express written permission of LM-ERCO. If you are a vendor of LM-ERCO, you are not to disseminate this information to any other person without the express written permission of LM-ERCO. If you are a customer of LM-ERCO, you are not to disseminate this information to any other person without the express written permission of LM-ERCO. If you are a licensee of LM-ERCO, you are not to disseminate this information to any other person without the express written permission of LM-ERCO. If you are a partner of LM-ERCO, you are not to disseminate this information to any other person without the express written permission of LM-ERCO. If you are a joint venturer of LM-ERCO, you are not to disseminate this information to any other person without the express written permission of LM-ERCO. If you are a member of LM-ERCO, you are not to disseminate this information to any other person without the express written permission of LM-ERCO.



1-GWh DIURNAL LOAD-LEVELING SUPERCONDUCTING MAGNETIC ENERGY
STORAGE SYSTEM REFERENCE DESIGN

APPENDIX A
ENERGY STORAGE COIL AND SUPERCONDUCTOR

by

R. I. Schermer

ABSTRACT

The technical aspects of a 1-GWh Superconducting Magnetic Energy Storage (SMES) coil for use as a diurnal load-leveling device in an electric utility system are presented. The superconductor for the coil is analyzed, and costs for the entire coil are developed.

I. INTRODUCTION

This appendix presents the details of the conceptual design for the coil and conductor of a 1-GWh Superconducting Magnetic Energy Storage (SMES) unit. The choices for total stored energy, coil shape, operating field, and operating current are discussed and justified. Once these free variables are chosen, the remainder of the coil parameters follows immediately and is given in Table A-I.

The proposed conductor is a 50-kA superconducting cable sandwiched between two parallel stabilizing elements, consisting of high-purity aluminum, jacketed with cold-worked copper for mechanical protection. Cable parameters are given in Table A-II. The allowable current density in the aluminum is set by coil protection considerations. Heat transport to the 1.8 K, 1-atm coolant is

discussed, and coolant channel dimensions are selected so that heat transfer at the conductor surface limits the allowable Joule heating in the conductor.

TABLE A-I
PARAMETERS FOR 1-GWh COIL

Overall Parameters

Average coil radius	66 m
Height	44 m
Radial thickness	0.30 m
Inductance	3170 H
Number of turns	4280
Winding pattern	pancake
Number of radial turns	5
Number of axial layers	856

Parameters of Axial Current Blocks

<u>Block Number</u>	<u>Turns</u>	<u>Axial Height, m</u>	<u>Mean Axial Position, m</u>	<u>Axial Turns/meter, m⁻¹</u>
1	970	8.8	0	22.0
2 and 3	476	4.4	+ 6.6	21.6
4 and 5	235	2.2	+ 9.9	21.4
6 and 7	210	2.0	+ 12.0	21.0
8 and 9	200	2.0	+ 14.0	20.0
10 and 11	94	1.0	+ 15.5	18.8
12 and 13	91	1.0	+ 16.5	18.2
14 and 15	89	1.0	+ 17.5	17.8
16 and 17	87	1.0	+ 18.5	17.1
18 and 19	71	1.0	+ 19.5	14.3
20 and 21	65	1.0	+ 20.5	13.0
22 and 23	37	1.0	+ 21.5	7.4

TABLE A-II
 PROPERTIES OF 50-kA SUPERCONDUCTING COMPOSITE CABLE

Design J_c at 1.85 K, 5.2 T, $10^{-14} \Omega\text{-m}$	$3.3 \times 10^9 \text{ A/m}^2$
Alloy	Nb-46.5 wt% Ti
Operating current	50.0 kA at 4.7 T
Design critical current	55.6 kA at 5.2 T

Strand Parameters

Design critical current	2417 A
Number of filaments	1490
Filament diameter	25 μm
Cu-to-NbTi ratio	1.33
Diameter	0.147 cm
Twist pitch	1.5 cm

Cable Parameters

Number of strands	23
Packing factor	0.85
Dimensions	0.277 cm by 1.67 cm
Transposition length	16.0 cm
Mass per meter	0.29 kg/m

After a consideration of magnetoresistance and cyclic-strain effects, the aluminum purity is specified. The final conductor design is given in Tables A-II and A-IV.

AC losses in the conductor are considered next and shown to be nominal, with the possible exception of frictional losses due to the relative motion of various coil components. This latter must be carefully controlled by proper coil construction. It is also shown that eddy current heating in the steel helium vessel will be extremely large unless the vessel contains an insulating section so that it does not act like a large conducting ring.

For reference design purposes the coil is constructed by placing individual radial and axial spacers between the conductor turns as the magnet is being wound. The mechanical design and cost of these spacers are considered in the final section.

II. TOTAL STORED ENERGY AND DISCHARGE RATIO

The energy, E , to be exchanged with the electric utility has been specified as 1 GWh; but the energy, W_{\max} , actually stored in the magnetic field when the coil is fully charged has not been specified, nor has W_{\min} . The three quantities are related by

$$E = W_{\max} - W_{\min} \quad .$$

The discharge ratio, ϵ , is defined by the equation

$$\epsilon^2 = W_{\max} / W_{\min} \quad ,$$

then

$$\frac{E}{W_{\max}} = \frac{\epsilon^2 - 1}{\epsilon^2} \quad .$$

The dc current and magnetic field at the limits of the charge-discharge cycle are related to ϵ by

$$\frac{B_{\max}}{B_{\min}} = \frac{I_{\max}}{I_{\min}} = \epsilon \quad .$$

If a SMES system is required to supply constant power to the utility grid, the ratio of coil terminal voltages at the limits of the cycle is also given by

$$\frac{V_{\max}}{V_{\min}} = \epsilon \quad .$$

The installed converter power is independent of V_{\max} for $2 < \epsilon < 5$. A value of $\epsilon = 3.33$ is chosen as a reasonable compromise, because for any value of ϵ greater than approximately three, the coil size decreases but little with ϵ , whereas the terminal voltage increases greatly.

III. OVERALL COIL DESIGN

Choices for magnet shape have been considered in detail in previous work.^{1,2} A thin-walled solenoid is least expensive in terms of superconductor and easiest to support mechanically but creates a rather large external field compared to a toroid. Options for using a guard coil are discussed in Chap. VIII³ and Ref. 1. A simple solenoid, as shown in Fig. A-1, is specified by three parameters: (a) the average radius, (b) the height, and (c) the radial thickness. For convenience, two ratios, $\alpha = c/2a$ and $\beta = b/2a$, are defined. In previous cost optimization studies, a broad cost minimum about $\beta = 1/3$ is found, which is the value used here.

The operating magnetic field is also a result of a cost optimization procedure.¹ A low field leads to more efficient superconductor use, lower capital cost for struts and refrigerator, and lower operating costs for refrigerator power. The cost of normal-conductor stabilizer changes very slowly with field; the details depend upon the magnetoresistivity of the stabilizer material. The sharpest field dependence, however, is that of the dewar, whose cost decreases dramatically with higher fields. The overall result is that the total cost tends to be very flat over a range of fields from 3 to 7 T even though there is a wide variation of unit costs for the various elements. If cold support is used, rather than warm support, the cost decreases slowly over the same field range. For the first iteration, a value of 4.5 T was chosen. The coil radius, a , was then fixed by the requirement that a single-layer solenoid with uniform current density and $\beta = 1/3$ would store energy W_{\max} with a maximum field, B_{\max} , at the winding of 4.5 T.

$$W_{\max} = \frac{B_{\max}^2}{2 \mu_0} f(\beta) a^3 \quad ,$$

where the factor $f(\beta)$ was obtained by numerical computation. The design then evolved through several iterations and stages of complexity in which the fixed parameters were taken as W_{\max} , β , the value of "a" just calculated, and a winding thickness of 30 cm. During the process, the values of B_{\max} remained in the range of 4 to 5 T; therefore, the adjustment of the value of "a" was unnecessary.

For a thin-walled solenoid $\alpha \rightarrow 0$, the magnetic field tends to peak sharply at the coil end unless the current density is allowed to vary with

axial position. A calculation was performed in which axial spacing of turns was varied in 24 discrete steps. This results in a magnetic field which is constant to within a few percent everywhere on the innermost conductor turns. The winding parameters from this calculation are given in Table A-I. There is no correlation between the height of the various current blocks in Table A-I and the height of the segments into which the coil is mechanically divided for stress reasons. The design is purely illustrative. A further iteration will be necessary because "c" will change significantly from its assumed value, and the current blocks will have spaces between them.

IV. MAXIMUM CURRENT AND TERMINAL VOLTAGE

The power rating of a SMES unit is determined by the application, but the separate choice of current and voltage is one of engineering judgment. The installed converter cost is almost independent of voltage over a wide range covering typical power system practice. Possibly there is an optimum current which results in a minimum cost for the total system. At this point, reasonable power system voltage and current have been chosen for the reference design because industry must acquire considerable experience in the field construction of large coils before a valid optimization can be performed. For reference, several factors which can enter into an optimization are listed below.

- (a) The higher the current, the more difficult the conductor will be to handle physically. Thus, the conductor winding rate will be slower while the length of conductor to be laid down decreases inversely as the current. The cheapest coil may use the largest possible conductor.
- (b) The higher the current, the smaller the terminal voltage will be. One-half the terminal voltage appears between each magnet terminal and the grounded parts of the dewar. The maximum safe value for this potential difference to ground can only be conjectured. Superconducting power transmission line designs call for > 100 kV. For a 1-GWh 250-MW SMES unit to succeed, development must proceed to the point where voltages of at least 50 to 100 kV are allowable under either routine operation or fault conditions.
- (c) A drawback to high current is the extra refrigeration required by the power leads. Although this is a minor contribution for the main pair

of leads, it may be significant if multiple leads are required for protection.

- (d) At some sufficiently high current, a single layer coil that has certain mechanical advantages can be built. For this design, multilayer coils are considered together with the structural problems involved in their construction, rather than to limit the design to single-layer coils at this stage. A modular conductor probably can be constructed for a high enough current to allow single-layer construction if necessary. At this stage, conductors which cannot support stresses of the order of 10^8 MPa (15 ksi) in any direction seem extremely inconvenient to use in any coil design.
- (e) A small amount of stabilizer can be saved by running at a considerably lower current and correspondingly higher terminal voltage.

V. STABILITY AND PROTECTION

Stability refers to the capacity of a superconducting system to undergo a perturbation and maintain or regain the superconducting state. The proposed conductor is designed so that a long length of conductor may be driven well above its transition temperature and recover, that is, return to the superconducting state. The actual stability limit of the system is also determined by details of helium inventory and fluid flow which affect local helium replenishment in addition to the conductor properties.

A cryostable conductor can, in principle, carry a current density of more than 50 kA/cm^2 , which consequently reduces the cost of stabilizer to a trivial amount. Such a design would take advantage of the extremely good heat transfer available in liquid helium at 1.8 K and 1.0-atm pressure and the low electrical resistance in a magnetic field of high-purity aluminum.

In practice, however, the question of protection intrudes upon this idealized scheme. Protection is the process whereby the energy is removed from a coil to prevent damage from occurring. Damage may result from overheating and its attendant thermal stresses or from electrical breakdown. Three distinct types of events are generally cited as requiring protective action.

- (a) Design or construction flaws could lead to conditions requiring emergency action. This is the most common historical reason for coil failure. A proper engineering development program should reduce the probability of such occurrences.

- (b) The conductor could lose its cryostability so that if it went normal it would not recover automatically. Blockage of coolant channels is often cited as a possible hazard in this regard.
- (c) Unforeseen conditions such as refrigerator failure or vacuum leaks might force emergency action.

Protection involves providing sufficient time to discharge the coil energy; the time is lengthened by lowering the current density in the conductor stabilizer and hence raising the stabilizer volume. This process becomes prohibitively expensive if it is thought necessary to discharge the entire coil at a modest turn-to-turn voltage. Clearly it is necessary to perform a cost-benefit analysis on a protection system. To perform such a calculation the probabilities and consequences of various failure modes must be known.

The present level of design leaves some uncertainties to be resolved. A design that attempts to account for all current unknowns may be unrealistically conservative by a large factor. To ignore the protection problem is certainly optimistic. A middle course, in which an emergency requires protecting only one segment of the magnet, is postulated. If 1% of W_{\max} is to be removed with a turn-to-turn voltage of 100 V/turn, the maximum allowable current densities are 21 kA/cm² in copper or 15 kA/cm² in aluminum. The stability analysis must then be used to determine if such current densities can indeed be tolerated. The answer depends greatly upon the details of the cryogenic and structural design. Under the assumptions that will be made, copper cannot be operated readily at this high a current density; and there is no great cost advantage for running aluminum at so high a density. Reducing the current density is worthwhile, and it eases the protection problem.

VI. CONDUCTOR DESIGN

A. General Considerations

The conductor should be fully cryostable, exhibit modest ac losses, should be able to be fabricated in relatively long lengths and to be wound in place underground, and should support a reasonable stress level. The conductor chosen is stabilized by aluminum with its current density set at 15 kA/cm² for protection reasons. A sample of copper-jacketed, aluminum-stabilized conductor of the type specified here has been prepared by Airco Superconductors, Inc. for the SMES program. Results of a cost study on high-purity aluminum, performed by Alcoa, are given in Appendix B.⁴

For convenience in fabrication and handling, the conductor consists of two parallel elements in electrical contact sandwiched about a 13-strand superconducting composite cable. Such a modular design would allow grading the quantity of superconductor and the shape and quantity of stabilizer as a function of location. This would result in significant material savings in these elements as well as in the interturn spacers.

B. Superconductor Design

Cable parameters are given in Table A-II. The conductor is sized to operate at 90% of the short-sample critical current along the maximum field load line in the coil. If the critical current is measured at $1 \times 10^{-14} \Omega\text{m}$, there will be at least an additional 10% safety margin in the magnet operation in that the Joule heating will be unnoticeable at this resistance level. Thus, each cable strand must operate at 2.17 kA at 4.7 T but is sized to carry 2.42 kA at 5.2 T.

The appropriate value of expected critical current density at 1.85 K must be calculated. There are few data for guidance nor is there a sufficiently accurate theory. In general

$$J_c(T) \propto 1 - \left(\frac{T}{T_c} \right)^n, \quad (\text{A-1})$$

where n is of the order of 1 to 2. The data of Hancox shows that $J_c(1.85)/J_c(4.2) = 1.6$ at 3 T, for which $T_c = 7.8$ K. From Eq. (A-1), the ratio is expected to lie between 1.32 ($n = 2$) and 1.65 ($n = 1$). The data thus lie rather close to a linear relation, as do data above 4.2 K. With $n = 1$ and $T_c \approx 7.0$ K, corresponding to 5 T,

$$\frac{J_c(1.85 \text{ K})}{J_c(4.2 \text{ K})} = 1.84 \text{ at } 5 \text{ T.}$$

The ratio might be even higher for an alloy whose fabrication is optimized for the specified conditions. For a typical value of $J_c(4.2 \text{ K}, 5.2 \text{ T}) = 1.8 \times 10^9 \text{ A/m}^2$, $J_c(1.85 \text{ K}, 5.2 \text{ T}) = 3.3 \times 10^9 \text{ A/m}^2$. With a Cu-to-NbTi ratio of 1.33, the composite area is small enough that a monolith could be used, but a monolith does not allow the amount of superconductor to be varied simply as a function of position. The superconducting composite should be

mounted on a vertical face of the stabilizer where it is subject only to the modest radial compressive stress, rather than on a horizontal face where it must support the large axial stress. It also yields smaller ac losses when mounted vertically. For these reasons a 23-strand cable, to be set into shallow channels in the stabilizer faces, is specified with an aspect ratio of six.

The strand called for in Table A-II is typical of those presently being produced commercially. A single extrusion billet yields at least 180 kg or 14 000 m of strand in several long lengths. Cable is typically fabricated from random lengths cold welded together, with the cold welds staggered along the cable length, so that there is little waste and no maximum length restriction.

The coil requires 1.77×10^6 m of 55.6-kA conductor or 9.9×10^7 kA-m of conductor. From Table 4.2 of Ref. 5, the composite can be estimated to cost \$1.10/kA-m at 4.2 K and 5 T and hence should cost \$0.60/kA-m at 1.85 K and 5 T. The total price of the composite strands is then \$59.3 million, or a saving of \$41.6 million over the cost if the coil were to operate at 4.2 K. There is an additional cost of \$0.60/m of 23-strand cable for cabling, or \$1.06 million.

The above design puts far too much superconductor in the low-field regions of the coil. Approximately 29% of the superconductor could be eliminated if the Cu-to-NbTi ratio was adjusted so that just enough NbTi alloy is located at every position to operate at 90% of critical current. The most straightforward way to do this is to replace composite cable strands by pure copper strands. This replacement also disrupts the perfect cable transposition and results in nonuniform current distribution among the strands. A second alternative is to fabricate cable strands with ten different Cu-to-NbTi ratios, which could be phased into the cable as desired. The overall composite conductor cost is thus estimated at 71% of the previously quoted value, or \$42.1 million for the strands plus \$1.06 million for cabling.

There is considerable margin for decrease in the above composite price, which represents a cost of \$350/kg of contained NbTi compared to the current price of \$100/kg for the alloy as fabricated into rods ready to be stacked and extruded. The coil will require roughly 2800 extrusion billets, compared to the largest order the industry has previously processed of 100 billets for the Fermi National Accelerator Laboratory (FNAL). This represents a considerable margin for development to reduce the cost of the finished conductor.

VII. CRYOGENIC DESIGN CONSIDERATIONS

A. Introduction

The conductor must recover from perturbations which drive it normal by transferring heat to the liquid helium. There are two mechanisms which limit the steady-state heat removal capacity. First, there is a maximum heat flux that can leave a surface. The assumption is usually made that the maximum value is set by the peak nucleate boiling flux (PNBF), although this assumption is in fact quite conservative for localized perturbations. The PNBF in He II at 1 atm is at least 5 W/cm^2 . A limit of 5 W/cm^2 is assumed for this design. A second condition is set by the limiting heat flux, q_ℓ , in the coil cooling channels. Experiments have verified that q_ℓ is a function of the channel length, ℓ . If ℓ is measured in centimeters, then

$$q_\ell = \frac{q_1}{\ell^{1/3}} \text{ W/cm}^2, \quad (\text{A-2})$$

where q_1 , the limiting flux in a channel 1 cm long, is a function of the temperature at the cold end of the channel and of the bath pressure, and is approximately $7.5 \text{ W/cm}^{5/3}$ for a bath at 1.85 K and 1 atm. Because the total heat which can be carried by a channel is found by multiplying q_ℓ by the cross-sectional area of the channel, narrow, internal channels between subconductors make a negligible contribution to heat transport when compared to the far wider channels between coil turns. Thus, internal channels have been completely eliminated in the conductor design.

If more than one conductor adjacent to a particular channel should become normal, the allowable heat generation rate from each conductor would have to be reduced because the channel could carry away less heat from each conductor. This condition affects the economics because it requires use of a higher purity aluminum. Such an event is too unlikely to be used as a design basis. A conductor is presumably driven normal by a local perturbation that causes a few meters of conductor to be in the normal state for a few hundred milliseconds. In a properly designed coil this would be a rare occurrence and the chance of its happening in two adjacent conductors should be even more rare. Further, the limitation of the maximum design heat flux to the value, which can be carried without a transition to film boiling, is also

conservative. Thus, the cryogenic design will only consider an event in which one isolated length of conductor must recover.

Equation (A-2) represents the experimental data for a single, fluid-filled channel, but it is not known how it applies to a coil in which there are multiple, interconnected channels between the presumed normal conductor and the bulk of the He II liquid. The assumption is made that, once the heat has left the immediate vicinity of the conductor, there are so many parallel heat conduction paths that the winding effectively acts like an open bath. Eventually, however, experiments must be performed on a mockup of the structure.

The detailed geometric arrangement of the conductors affects cost both through its effect upon heat transfer and upon the structural design. The optimum design will most likely be different from that presented here but cannot now be determined because of a lack of experimental and cost data.

B. Channel Design

The channels will be made large enough so that the PNB_r at the conductor surface will be the controlling parameter. Consider the conductor array shown in Fig. A-2, in which the central conductor is assumed to be normal. From symmetry considerations only one-quarter of the conductor, which carries 12.5 kA in a block of stabilizer of vertical height w and radial thickness t , need be considered. The resulting Joule heating is

$$q_J = \frac{I^2 \rho}{A} = \frac{I^2 \rho}{wt} \text{ W/cm} \quad . \quad (A-3)$$

This heat is removed through a horizontal channel of height X'' and length t and a vertical channel of width X' and height w . Each channel is only open for a fraction, f , of its length into the plane of the figure with the remainder of the channel blocked by structural material. From Eq. (A-2), it follows that the maximum power which can be removed per centimeter of conductor by the horizontal channel is

$$q_H = \frac{7.5 X'' f}{t^{1/3}} \text{ W/cm} \quad ,$$

whereas for the vertical channel it is

$$q_V = \frac{7.5 X' f}{w^{1/3}} \text{ W/cm} \quad .$$

With the peak surface heat flux set at 5 W/cm^2 , the maximum power which can enter the horizontal channel per centimeter of conductor is

$$q'_H = 5 t f \text{ W/cm} \quad ,$$

and for the vertical channels

$$q'_V = 5 w f \text{ W/cm} \quad .$$

The requirements $q_H > q'_H$ and $q_V > q'_V$ lead to the conditions

$$X'' \geq 0.67 t^{4/3} \quad \text{and} \quad X' \geq 0.67 w^{4/3} \quad . \quad (\text{A-4})$$

Furthermore, with

$$q'_V + q'_H = q_J \quad , \quad (\text{A-5})$$

$$5f(w + t) \geq q_J \quad .$$

Axially, the coil turns are not required to be very close together even at the center of the coil, so there are horizontal spaces which must be filled in any event. See Table A-I. Suppose $w \gg t$ to assist in filling these spaces. Then Eq. (A-4) demands that the horizontal separation, X' , be large, so that otherwise extraneous material must be included in the vertical spacers. Also, the axial force must now be supported by the smaller bearing surface, t , which may require a larger fraction, f , of the horizontal channels to be obstructed.

Another option would be to make $t \gg w$. This requires narrow vertical channels with a saving on extraneous material and large horizontal channels, which exist anyway. To the extent that the horizontal channels would be larger than necessary, this again represents extraneous spacer material. Now,

however, the bearing load is more widely distributed, which might allow a larger fraction of the channel to be left open.

To obtain numerical results for minimum channel sizes, the value of q_J will be calculated in the following section.

C. Stabilizer Design

If the conductor aspect ratio, ξ , is defined by

$$\xi = \frac{w}{t} \quad , \quad (A-6)$$

then Eqs. (A-3), (A-5), and (A-6) yield a relation between the conductor dimensions and the required resistivity which is

$$t^3 \geq \frac{I^2 \rho}{5 (1 + \xi) f} \quad . \quad (A-7)$$

For the present design, a square conductor with $\xi = 1$ is used, although it is likely economic optimization may require a different value.

Equation (A-7) also implies a maximum value of current density for a given ρ and ξ . For $\xi = 1$ the relation becomes

$$J = \frac{I}{t^2} = \left(\frac{10 f}{\rho} \right)^{2/3} I^{-1/3} \quad . \quad (A-8)$$

Table A-III gives the conductor dimension and resistivity for various values of J and f as calculated with Eqs. (A-7) and (A-8).

For annealed oxygen-free copper at 4.7 T, $\rho = 2.2 \times 10^{-8} \Omega \text{ cm}$. Since this material has a yield strength of only 10 ksi at 4.2 K, a more useful stabilizer might be given 5 to 7% cold work. Cold work raises the yield strength to > 30 ksi but only raises the resistivity to $2.97 \times 10^{-8} \Omega \text{ cm}$. Table A-III reveals that in either case, with $f \approx 0.5$, as will probably be required in the most highly stressed coil regions, it will be necessary to operate a copper-stabilized coil at $< 15 \text{ kA/cm}^2$. That is, for copper it is more difficult to meet the heat transfer requirement of Eq. (A-5) than the protection requirement. For aluminum the resistivities given in Table A-III are perfectly reasonable and there seems to be a sizable cost advantage in using aluminum, at least in terms of the raw materials involved.

D. Properties and Costs of Stabilizing Materials

Table A-III gives the overall current density and the resulting required value of ρ for the conductor. It is still necessary to calculate J and ρ separately for the aluminum and the copper jacket.

The relations

$$(J\rho)_{Al} = (J\rho)_{Cu} = J\rho \quad (A-9a)$$

and

$$JA = \sum_i (JA)_i \quad (A-9b)$$

imply that

$$\frac{A}{\rho} = \sum_i \left(\frac{A}{\rho} \right)_i \quad (A-9c)$$

The assumption is made that $A_{Cu}/A = 0.2$ and $A_{Al}/A = 0.8$, which corresponds to the smallest copper fraction that Airco has yet attempted to fabricate, and $\rho_{Cu} = 2.97 \times 10^{-8} \Omega \text{ cm}$. There remains one free variable among ρ_{Al} , J_{Al} , and J_{Cu} .

TABLE A-III

DESIGN PARAMETERS FOR A 50-KA CONDUCTOR MODULE

J kA/cm ²	t cm	f	ρ 10 ⁻⁸ Ω -cm
20	0.791	0.50	1.58
		0.66	2.11
		1.0	3.16
15	0.913	0.50	2.44
		0.66	3.24
		1.0	4.87
10	1.12	0.50	4.47
		0.66	5.96
		1.0	8.94

The cross-sectional area of stabilizer required is proportional to $1/J$ and, therefore, to $\rho^{2/3}$. The average price of high-purity aluminum is expected to vary approximately as $\rho^{-0.6}$. The total cost of aluminum stabilizer is, therefore, expected to decrease only very slowly with resistivity; thus the

$$\text{Cost of Al} \sim \rho^{0.07} .$$

This implies that there is no great economic advantage in running an all-aluminum coil at the maximum J allowed by protection considerations. By contrast, the cost per kilogram of copper stabilizer is essentially independent of its resistivity so that a copper stabilizer will be cheapest when run at its maximum J . For the copper-jacketed aluminum stabilizer, the situation is rather more complex. The copper area is given by

$$A_{Cu} = 0.2 A = 0.2 \frac{I}{J} .$$

The copper area and hence the copper cost will thus be minimized by maximizing J consistent with all the other constraints in the problem. For the particular case chosen, the limiting condition is $J_{Al} = 15 \text{ kA/cm}^2$. The operational parameters of the conductor are now fully determined and are given in Table A-IV. The conductor is shown in Fig. A-3.

The cost of aluminum depends upon its residual resistivity ratio (RRR) in the unstrained, zero-field condition. Segal⁶ has shown that a cyclic-tensile strain of 0.1% produces a change of 20% in the RRR of high-purity aluminum within the first thousand cycles and little change thereafter. In the current application, the material is being compressed axially while being restrained radially and longitudinally, and it is likely that a stress-strain curve will be virtually linear for strains up to and beyond 0.1%. Only small energy losses are expected from mechanical hysteresis with perhaps only minor changes in RRR. Clearly, experimental work is necessary to resolve these matters. Meanwhile, a maximum tolerable strain of 0.1% in the aluminum and a corresponding increase of 20% in the electrical resistivity are assumed. The results of Fickett⁷ indicate that the resistivity in a field of 4.7 T is approximately 2.6 times that in zero field for an initial RRR of 1000. The assumption is made that the aluminum in the conductor will have its

TABLE A-IV

OPERATIONAL PARAMETERS OF A 50-kA STABILIZER

Dimensions	1.856 cm by 1.856 cm
Aluminum dimensions each side	0.80 cm by 1.73 cm
Copper jacket thickness	0.065 cm
Volume fraction aluminum	0.8
J	14.5 kA/cm ²
J _{Al}	15.0 kA/cm ²
J _{Cu}	12.5 kA/cm ²
ρ	2.56 x 10 ⁻⁸ Ω cm
ρ_{Al}	2.47 x 10 ⁻⁸ Ω cm ^a
ρ_{Al}	7.97 x 10 ⁻⁹ Ω cm ^b
ρ_{Cu}	2.97 x 10 ⁻⁸ Ω cm
Mass of aluminum in magnet	1.27 x 10 ⁶ kg
Mass of copper in magnet	1.05 x 10 ⁶ kg

^aAs cyclically strained at 4.7 T.

^bUnstrained in zero field.

resistivity increased by an overall factor of $1.2 \times 2.6 = 3.1$ from its original value. The original aluminum, therefore, is required to have a resistivity of less than $7.97 \times 10^{-9} \Omega$ cm or an RRR of 340. From the Alcoa study the average price of aluminum is estimated to be \$4.50/kg, compared to \$1.50/kg for copper. The total material costs become \$5.7 million for aluminum and \$1.6 million for the copper jacket.

Two final points are made about protection. First, the temperature integral of the specific heat divided by the resistivity should be recalculated for the copper-jacketed aluminum conductor. This would probably result in different limits on J and would require a second iteration to calculate ρ_{Al} . Second, J_{Al} could be reduced significantly below 15 kA/cm² with only a modest increase in conductor cost. For instance, if J_{Al} = 10 kA/cm², then J = 10.9 kA/cm², $\rho = 3.92 \times 10^{-8} \Omega$ cm, and $\rho_{Al} = 4.26 \times 10^{-8} \Omega$ cm (RRR = 197). The cost for aluminum is virtually unchanged, whereas that for the copper jacket is increased by \$0.5 million. The incremental cost for the finished, installed conductor could be so small

as to be more than canceled by a savings in the costs associated with protection.

E. Conductor Stability

All the numbers needed to demonstrate stability are now available. From Eq. (A-3) the Joule heating for each quadrant of the 50-kA conductor is given by

$$q_J = \frac{I^2 \rho}{A} = (1.25 \times 10^4)^2 \times 2.56 \times 10^{-8} / (0.928)^2 = 4.64 \text{ W/cm},$$

whereas, from Eq. (A-5) the allowable heat flux per centimeter of conductor length is

$$q_V + q_H = 5f(w + t) = 5(0.5)(0.928 + 0.928) = 4.64 \text{ W/cm} \quad .$$

From Eq. A-4 the surface heat flux will be the limiting condition provided the channel widths are given by

$$x'' = x' \geq (2/3)w^{4/3} = 0.60 \text{ cm} \quad .$$

VIII. CONDUCTOR LOSSES

A. Hysteretic Loss

During a charging cycle, the field at position r within the conductor changes from $B_{\min}(\bar{r})$ to $B_{\max}(\bar{r})$. This results in an energy loss from hysteresis within the superconducting filaments of diameter d given by

$$Q_h = \frac{2}{3\pi} d \int \lambda(r) dV \int_{B_{\min}(\bar{r})}^{B_{\max}(\bar{r})} J_c(B) dB \left[1 + (I/I_c)^2 \right] \quad , \quad (\text{A-10}).$$

and a corresponding power loss, $P_h = Q_h/T$. The space factor, λ , is defined by

$$\lambda = \frac{A_{sc}}{A_{cond}} \quad ,$$

and the volume integral is taken over the conductor volume rather than over only the superconductor volume. In most coils $\lambda = \text{constant}$, and the volume integrals must be evaluated numerically. Here, however, the amount of superconductor has been arranged at every position so that $\lambda(\vec{r})J_c(B)$ and, thus, (I/I_c) are independent of position and equal to their values at the maximum field position. If these quantities are written as $\lambda_M J_c(B)$ and $(I/I_c)_M$ respectively, then Eq. (A-10) becomes

$$Q_h = \frac{2}{377} d\lambda_M V_c \int_{B_{\min}}^{B_{\max}} J_c dB \left[1 + (I/I_c)_M^2 \right], \quad (\text{A-11})$$

where the field integral now refers to the maximum field point, and V_c is the conductor volume. Note that $\lambda_M V_c$ is the superconductor volume which would have been present if the superconductor area had not been graded. The J_c and I_{cM} at any field can be written in terms of their specified values at 5.2 T from Table A-II and by using the Kim-Anderson formula

$$J_c(B) = 3.3 \times 10^9 \left(\frac{5.2 + B_0}{B + B_0} \right) \text{ A/m}^2$$

and

$$I_{cM}(B) = 5.56 \times 10^4 \left(\frac{5.2 + B_0}{B + B_0} \right) \text{ A}.$$

Also, at the maximum field point, $B = 9.4 \times 10^{-5} \text{ T}$.

The integral may be evaluated analytically. Numerical values for Q_h and the corresponding power, P_h , are given in Table A-V. These values depend somewhat upon B_0 , which in turn seems to depend upon the detailed heat treatment schedule during wire fabrication. A relatively low value of $B_0 = 0.20$ has been used, which leads to a conservatively large value of Q_h . If $B_0 = 1.0$ had been assumed, then Q_h would have been reduced by 9%.

B. Self-Field Loss

The filaments within a cable strand are fully transposed with respect to the total field generated by the magnet but are not transposed with respect to the self-field generated by the strand itself. This produces a nonuniform

current distribution among these filaments and an additional source of hysteretic loss which, following Wilson, is

$$Q_s = \eta \frac{\mu_0 I^2}{2\pi^2 D^2} V_s \quad , \quad (A-12)$$

where I and D are the current and diameter of one strand in the cable and V_s is the volume of the strands. See Table A-II. The η depends upon the magnetic history of the specimen and upon (I/I_c) ; it equals unity for the initial coil charge but is reduced to 0.1 for the second and subsequent charge-discharge cycles.

C. Coupling Loss

Coupling currents are eddy currents which flow longitudinally in the superconductor and transversely through the copper matrix. Because the rms value of the radial component, B_r , of the magnetic field is roughly one-third the rms value of the axial component, B_z , the loss can be minimized by placing the composite cable with its wide face vertical, that is, normal to B_r .

TABLE A-V
CALCULATED AVERAGE ELECTRICAL LOSSES IN THE 1-GWh COIL
FOR THREE CONDITIONS

<u>During 4-h Charge or Discharge</u>	<u>Watts</u>
Hysteresis, P_h	215
Self-field, P_s	22
Coupling, P_c	0
Eddy currents, P_E (conductor)	2
Eddy currents, P_E (dewar)	3
Joints, P_j	61
<u>While Holding Full Charge</u>	
P_j	131
$P_h = P_s = P_c = P_E = P'E$	0
<u>While Holding Minimum Charge</u>	
P_j	12
$P_h = P_s = P_c = P_E = P'E$	0

A formula for this energy loss per unit volume of cable, $\Delta Q_{c1}/\Delta V$, has been given by Wilson as

$$\frac{\Delta Q_{c1}}{\Delta V} = \frac{\Delta B_r \dot{\Delta B}_r p^2}{120 \rho_c} \left(\frac{w'}{2}\right)^2 \frac{w'}{t'} \quad (A-13a)$$

The cable has dimensions w' and t' ($w' > t'$), twist pitch p , and transverse resistivity ρ_c , whereas the conductor is a square, $2t$ on a side. The appropriate dimensions are given in Tables A-II and A-IV, whereas the value of ρ_c appropriate to $25 \mu\text{m}$ filaments has been measured as $\rho_c = 5 \times 10^{-10} \Omega\text{m}$, almost independent of field. The axial field contribution similar to Eq.(A-13a) is negligible. There are, however, additional contributions from shunting currents which flow through the stabilizer. Formulae, derived by Turck⁸ for these losses, are

$$\frac{\Delta Q_{c2}}{\Delta V} = \frac{\Delta B_r \dot{\Delta B}_r p^2}{24 \rho_1} \quad (A-13b)$$

and

$$\frac{\Delta Q_{c3}}{\Delta V} = \frac{\Delta B_z \dot{\Delta B}_z p^2}{128 \rho_2} \left(\frac{t'}{w'}\right)^2, \quad (A-13c)$$

where $\Delta Q_{c2}/\Delta V$ and $\Delta Q_{c3}/\Delta V$ are the energy losses per unit volume caused by radial and axial fields, respectively, and ρ_1 and ρ_2 are effective resistivities of the current paths. Both ρ_1 and ρ_2 must be of the order of the stabilizer resistivity, ρ . The three components must be averaged over the coil volume and must include the magnetic field variation of the various resistivities. The three components make fractional contributions to the final total of 0.58, 0.41, and 0.01 for Eqs. (A-13a), (A-13b), and (A-13c), respectively.

D. Eddy Current Loss

Eddy current loss in the stabilizer is given approximately by

$$\frac{\Delta Q_E}{\Delta V} = \frac{\Delta B \dot{\Delta B} R_e}{4\rho}, \quad (A-14)$$

where R_e is an effective radius of the stabilizer defined so that $\pi R_e^2 = A$ where A is the cross-sectional area of the stabilizer. Again, Eq.(A-14) must be averaged over the coil volume.

Eddy current losses in the coil structure represent, potentially, a far more serious problem. The eddy current loss in a ring of material of radius a and volume V is given by

$$P_E = \frac{\dot{\phi}^2 V}{4\pi^2 a^2 \rho} \quad (A-15)$$

The ϕ is the total flux threading the plane of the ring, which may be calculated from the coil inductance by the relation

$$\phi = \frac{LI}{N} \quad (A-16)$$

The resistivity of stainless steel at 1 to 4 K is $67 \times 10^{-8} \Omega\text{m}$, and the volume of steel in the dewar is 650 m^3 , so that $P_E = 1.8 \times 10^4 \text{ W}$. Thus each dewar must contain an insulating section so that it does not act like a large, conducting ring. In that case, the flux in Eq.(A-15) becomes that which actually passes through the steel, and the formula reverts to that shown in Eq.(A-14) for each element of the dewar, with R_e a characteristic dimension of that element. This may be the height, width, or thickness depending upon whether the dewar sides or top are considered and whether the calculation involves B_r or B_z . The value given in Table A-V is a very rough estimate.

E. Joint Losses

Electrical joints will be necessary at both the inside and outside turns of the pancake coils, because a true double pancake would be very unwieldy to wind. There will be 857 joints including the end connections. At each joint half the stabilizer would be removed from each of the two conductors, the exposed composite cable would be soldered together with a 1-m overlap, and the conductor then would be mechanically clamped and braced. The current must transfer through two resistances in series.

1. The copper stabilizer in the composite strands, which is taken to have an RRR of 50 and an average path length equal to a strand diameter.

2. The solder layer, which is assumed to have a thickness of 0.1 mm and a resistivity of $5 \times 10^{-9} \Omega\text{m}$, corresponding to 60 Pb-40 Sn solder. With these assumptions the two contributions to the resistivity are equal. It is further assumed that each strand in the cable can transfer current over the entire length of the joint because of the shunting effect of the copper-aluminum stabilizer. Each joint is then found to have a resistance of $6 \times 10^{-11} \Omega$. The resultant Joule heating must be averaged over the daily cycle of the coil.

F. Mechanical Losses

There are two possible, distinct sources of mechanical irreversibility in the proposed design. First, many elements are mechanically inhomogeneous, anisotropic systems with internal strains arising from fabrication and differential thermal contraction. They may show nonlinear stress-strain relations and hysteresis. Experiments show that 316 stainless steel exhibits no mechanical hysteresis provided it is cycled in the elastic range and that this is true for both annealed material and material containing 0.7% plastic strain. The proposed design keeps all the components well within their elastic limit, but it remains to be shown experimentally if the losses would in fact be zero in that case for all the materials. Second, mechanical losses may arise from the relative motion of various coil components with frictional effects, and the design should minimize such motion.

IX. COIL WINDING

As presently conceived, the coil will be formed of 856 pancakes, each with five radial turns in thickness, with electrical joints at both the inner and outer radii. All pancakes will be wound from the outer radius to the inner radius, and successive pancakes must be alternately wound clockwise and counterclockwise. Radial spacers will be placed as each pancake is wound; axial spacers will be laid down before winding a subsequent pancake. An advantage of the proposed conductor is that it may be completely assembled in a factory and shipped to the winding site on a spool. This simplifies the necessary underground winding machinery and facilitates the task of grading the superconductor. Five turns of assembled conductor will have a mass of 3.32 metric tons and a length of $2.1 \times 10^3 \text{ m}$. The material should fit comfortably on a 4-m-diameter, 1-m-high winding spool as four layers with a total radial build of 7.5 cm. The spools themselves must be carefully wound with attention paid

to the layer-to-layer transitions at the ends. The winding machinery must be capable of supporting the spool, providing appropriate tension, restraighthening the conductor, forming the conductor to the proper ripple radius, and accurately guiding the conductor to the desired location. The winding machine can run on a track which later becomes part of the dewar structure.

If the conductor can be laid at 1 m/min, the winding task takes 3.0×10^4 h, or 3.4 yr of around-the-clock operation. This is almost certainly too long, because winding should proceed rapidly enough to stay ahead of the crews welding the dewars and installing plumbing, struts, and thermal insulation. Therefore, either the winding speed will have to be three to five times faster or several coil segments will have to be wound simultaneously.

If there is a crew of three per winding machine plus 50% for supervision, joint fabrication, and miscellaneous tasks, the job is found to take 1.35×10^5 man-hours at 1 m/min per crew. This effort costs \$2.7 million at \$20 per man-hour.

X. CONDUCTOR SUPPORT

If a single conductor is loaded axially, the vertical copper sidewalls bow outward; and the resultant bending stress limits the load-bearing capability of the conductor. In a coil, five conductor turns are laid side by side with intermittent radial spacers, so that adjacent turns provide support against bowing for all except the innermost and outermost walls of the entire pancake. In support Option 1, Fig. A-4, a thick band of support material is to be wound along these two surfaces to prevent bowing and also to help support the axial load. Once bowing is eliminated, the conductor can be designed for either maximum compression in the copper or maximum strain in the aluminum. This design is for a strain of 10^{-3} in the aluminum stabilizer, in which case the conductor will support 84 MPa (12.2 ksi) with a stress in the copper of 134 MPa (19.4 ksi).

Axial load is transmitted from pancake to pancake by spacer bars placed at the same angular increments as the radial spacer blocks and spanning the entire radial thickness of the pancake including the inner and outer support bands. Because the axial load accumulates within a dewar section, the amount of support material can also vary with position. Dimensions and stresses given immediately below are for the most heavily loaded pancakes. The axial

load on a pancake is shared by the conductor, radial spacer blocks, and support bands acting in parallel. The support elements must be high-modulus material to carry a significant share of the load; thus G-10 CR is not a suitable material. Stainless steel bands and blocks suitably covered with electrically insulating material are proposed. If the spacers are 0.6 cm thick radially and cover 50% of the conductor surface, then the support bands must total 5.0 cm in thickness. The outer band should be made much thicker than the inner one, so that it can share the tensile load. The compressive stress in the band will be 200 MPa (29.0 ksi).

The axial spacer bars are really just space fillers. Aluminum alloy, again covered with an electrical insulator, would seem to be the least costly material available for this service. For bars covering 50% of the pancake area, the compressive stress in the aluminum will be 240 MPa (35 ksi).

Table A-VI gives the volumes and fabricated prices for the various support elements. The cost of electrical insulation is not included. The rightmost column gives the cost for a graded structure, which is estimated to be 70% of an ungraded one.

TABLE A-VI
VOLUME AND COST OF CONDUCTOR SUPPORT ELEMENTS

OPTION I

<u>Element</u>	<u>Material</u>	<u>Unit Cost</u> \$/kg	<u>Volume, m³</u>	<u>Cost^a</u> \$10 ⁶	<u>Cost^b</u> \$10 ⁶
Radial spacer	S.S.	2.50	118	2.3	2.3
Support band	S.S.	2.50	331	6.5	4.5
Axial spacer	Al alloy	2.50	1040	7.1	5.0
			TOTAL	15.9	11.8

OPTION II

Radial spacer	Al alloy	2.50	118	0.8	0.8
Support band	Al alloy	2.50	146	1.0	1.0
Axial spacer	Al alloy	2.50	867	5.9	4.1
Axial support	S.S.	2.50	14	0.3	0.3
			TOTAL	8.0	6.2

^aAssumes equal structure at all positions.

^bStructure varies with position.

Although support Option I is straightforward to construct, it is rather expensive. Support Option II (Fig. A-4) can reduce the cost of internal structure by a large amount, although it adds complexity and an unknown cost to the dewar. The conductor stack is divided in half vertically, with the lower half resting on the dewar end and the upper half resting on a ledge attached to both the inner and outer helium vessel walls. The total force on each half-stack is now only slightly larger than the conductor itself can support. The bands and radial spacers can be made of aluminum alloy, coated with insulation, at a stress level of 73 MPa (11 ksi). The 14 layers of axial supports which rest directly upon the ledges must support a shear stress of 400 MPa (58 ksi), so they are made of steel rather than aluminum. Only an inner band is needed, since the outer helium vessel wall also acts as a support.

REFERENCES

1. R. W. Boom, Ed., "Wisconsin Superconductive Energy Storage Project," Vol. I and II, Engineering Experiment Station, College of Engineering, University of Wisconsin reports (1974 and 1976).
2. W. V. Hassenzahl, Ed., "Progress Report Superconducting Magnetic Energy Storage Project," Los Alamos Scientific Laboratory report LA-5472-PR (1973).
3. J. D. Rogers, W. V. Hassenzahl, and R. I. Schermer "1-GWh Diurnal Load-Leveling Superconducting Magnetic Energy Storage System Reference Design," Los Alamos Scientific Laboratory report LA-7885-MS Vol. I (1979).
4. C. N. Cochran, R. K. Dawless, and J. B. Witchurch, "1-GWh Diurnal Load-Leveling Superconducting Magnetic Energy Storage System Reference Design; Appendix B: Cost Study, High-Purity Aluminum Production," Los Alamos Scientific Laboratory report LA-7885-MS Vol. III (1979).
5. A. Petrovitch, M. S. Walker, B. A. Zeitlin, and J. D. Scudiere, "Final Report, Conductor for a 10-MWh Superconducting Magnetic Energy Storage Coil," IGC report 577-1, Intermagnetics General Corporation, Guilderland, NY, 1977.
6. H. R. Segal, "Reinforced Aluminum as a Superconducting Magnet Stabilizer," IEEE Trans. Magn. Mag-13, 109-11 (1977).
7. F. R. Fickett, "Magnetoresistance of Very Pure Polycrystalline Aluminum," Phys. Rev. B3, 1941 (1971).
8. B. Turck, "Losses in Superconducting Multifilament Composites under Alternating Changing Fields," Los Alamos Scientific Laboratory report LA-7639-MS (1979).

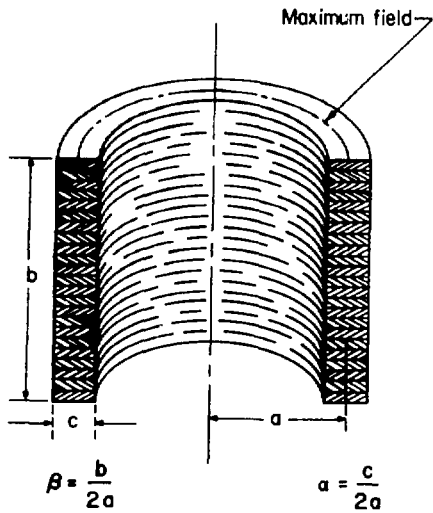


Fig. A-1.
Geometric variables of a simple solenoid.

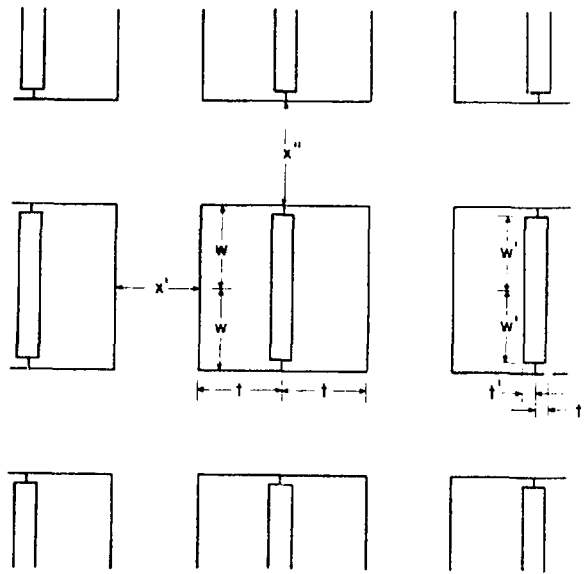


Fig. A-2.
Cross section of a conductor array,
showing geometric variables.

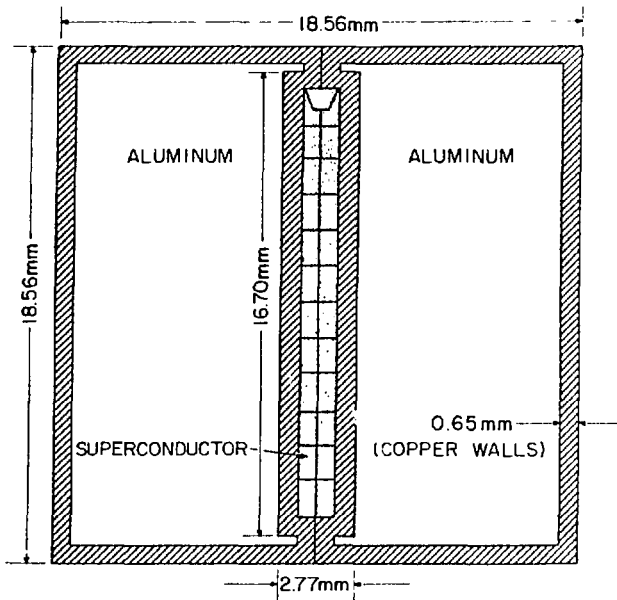


Fig. A-3.
Proposed 50-kA aluminum-stabilized
copper-jacketed conductor.

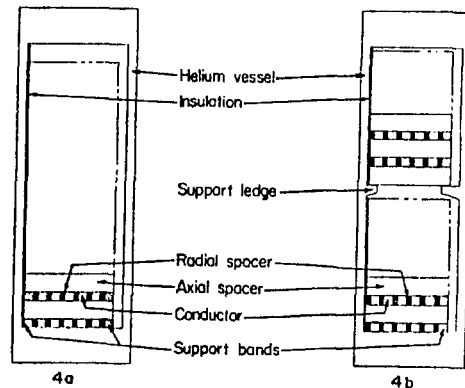


Fig. A-4.
Conductor support options. In Option I
(left), the axial load accumulates to
the bottom of the helium vessel. In
Option II (right), half of the axial
load is taken by the ledges.